Renewable Energy 134 (2019) 796–806

Contents lists available at ScienceDirect

Renewable Energy

journal homepage: www.elsevier.com/locate/renene

AGC of PV-thermal and hydro-thermal power systems using CES and a new multi-stage FPIDF-(1+PI) controller

Yogendra Arya

Department of Electrical and Electronics Engineering, Maharaja Surajmal Institute of Technology, Janakpuri, New Delhi, India

A R T I C L E I N F O

Article history:
Received 18 June 2018
Received in revised form
23 October 2018
Accepted 18 November 2018
Available online 19 November 2018

Keywords:
Energy system
Capacitive energy storage
Optimized FLC
Robust controller
Automatic generation control
PV system

A B S T R A C T

The interconnected power system with renewable energy sources is an intricate nonlinear system, which frequently brings to light the serious problem of the system frequency and tie-line power fluctuations due to deficient damping under severe and dynamically changing loading conditions. Primarily, the power system generation-demand equilibrium point amendments following a contingency and in this case, it is stiffer to recapture a tolerable equilibrium point via conventional control practices. To overcome this problem, advanced control techniques and fast acting energy storage systems (ESS) are requisite. The ESS such as capacitive energy storage (CES) units have tremendous capability in preserving the generation-demand balance and perpetuating the power grid frequency by effective damping of the power-frequency oscillations caused due to the sudden and variable load disturbances in power system. Hence, the impact of CES units in automatic generation control (AGC) of interconnected power system is analysed and contrasted critically in this paper. Motivated by the fact that fuzzy control techniques display superior performance under volatile operating conditions in contrast to conventional control strategies, this paper also proposes a new design of intelligent multi-stage fuzzy assisted PID with filter-(1 + PI) i.e., FPIDF-(1 + PI) controller to enhance the conduct of AGC of power system. Initially, a two-area photovoltaic-reheat thermal system is considered and the parameters of FPIDF-(1 + PI) controller are optimized utilising imperialist competition algorithm. The ascendancy of the proposed controller is substantiated by comparing the outcomes with PI/FPI/FPIDF controller based on various existing optimization techniques. It is observed that CES units installed in each control area sustain the area controller to restore the area frequency and tie-line power deviations adequately and hastily following a step load disturbance in an area. To exhibit the potency and scalability of CES and the proposed controller over other prevalent control methods, the study is also extended to a multi-unit multi-source hydro-thermal power system. Finally, robustness of the proposed controller with/without CES is validated under large changes in the system parameters and random load demands. Hence, the proposed approach asserts better and vigorous results to supply reliable and high-quality electric power to the end user.

1. Introduction

1.1. General

Maintaining the security, constancy and reliability of the power system is quintessential to get uninterrupted and quality electric power supply [1]. Frequency stability is a key index of power quality. Automatic generation control (AGC) plays a crucial role in spawning quality power in electricity system. AGC curtails the deviation in the system frequency and the tie-line power from the supposed values. These oscillations may be expanded and even lead to the system instability specifically in the presence of renewable energy sources (RES) like photovoltaic (PV) installations due to the lack of inertia and hydro plants due to the non-minimum phase characteristic of water turbine. In the modern fossil fuel-based power system, the integration of RES is rising due to the depletion of conventional sources, escalating fuel prices and environmental warming/pollution. However, in order to mix RES into such systems and to avoid frequency/power fluctuation, some form of energy storage or extra generation is generally desired [2].

The supplement of a small capacity energy storage system e.g., CES to power system and an effective AGC controller both can effectively enhance the quality of frequency/tie response. In order

E-mail address: mr.y.arya@gmail.com.

https://doi.org/10.1016/j.renene.2018.11.071
0960-1481/

Nomenclature

i	subscript referring to area-i ($i = 1, 2$)
P_{ri}	rated area capacity
α_{12}	area size ratio ($= P_{r1}/P_{r2}$)
F^0	nominal system frequency
R_i	speed governor regulation parameter
B_i	frequency bias constant
β_i	frequency response characteristics
K_{PSi}	power system gain
T_{PSi}	power system time constant
T_{Gi}	speed governor time constant
T_{Ti}	thermal turbine time constant
K_r	reheater gain
T_r	reheater time constant
T_{12}	tie-line synchronizing coefficient
T_{Ri}	hydro turbine speed governor reset time
T_{GHi}	hydro turbine speed governor main servo time constant
T_{Wi}	water starting time constant
T_{RHi}	hydro turbine speed governor transient droop time constant
ΔP_{gi}	incremental change in area power generation
ΔP_{Di}	incremental change in load demand in area
ΔP_{Gi}	incremental change in generating unit output
ps-i	power system
a/b/c/d	PV grid parameters
ACE_i	area control error

to preserve better quality of power supply, AGC should have robustness to the system parametric uncertainty and excellent load demand disturbance rejection aptitude. Hence, in addition to CES units, an advanced, intelligent and robust supplementary AGC controller is required to get desired dynamic performance of the power system.

1.2. Literature survey

As the fast acting energy storage devices like CES units act as add-on to the kinetic energy storage in the generator rotor moving mass, they can be used to effectively mitigate the electromechanical oscillations caused due to sudden load perturbations in power system [3]. The CES unit shares the sudden variation in power demand requirements for enhancement of the dynamic performance of an AGC system [4].

In the recent preceding decades, the ongoing concentration in the design of AGC strategies is detected to ensure enhanced performance of power system in normal and perturbated condition. The state-of-the-art literature surveys on various control approaches including the application of CES for AGC in traditional/restructured power system are presented critically in Refs. [5,6]. In order to attain a pleasing dynamic performance of AGC, a variety of conventional controller structures optimized via various intelligent soft computing techniques hitherto have been implemented for AGC of traditional/restructured power system like sine-cosine algorithm (SCA) based proportional integral (PI) [4], optimal control [7,8], model predictive control [9], population extremal optimization (PEO) based PI [9], craziness based particle swarm optimization (PSO) (CRAZYPSO) based PI [10], differential evolution (DE) based PI/PID [11,12], biogeography-based optimization (BBO) algorithm based I/PI/PIDF [13], disrupted oppositional based gravitational search algorithm (DOGSA) based PID [14], teaching learning based optimization (TLBO) algorithm based 2-degree of freedom (DOF) PID (2DOF-PID) [15], artificial bee colony (ABC) algorithm based PI/PID [16], hybrid gbest-guided gravitational search algorithm-pattern search (hGGSA-PS) algorithm based PID [17], firefly algorithm (FA) based PI/PID [18–20], hybrid FA PS (hFA-PS) technique based PI/PID [21], symbiotic organism search (SOS) algorithm based PID [22], imperialist competition algorithm (ICA) based PID [23] and hybrid stochastic fractal search-local unimodal sampling (hSFS-LUS) based multi-stage PDF-(1 + PI) [24] controllers.

The above passage reflects that the most extensively used controllers in AGC practice are the fixed gain type classical PI or PID controllers due to the benefits of simple and convenient structure. However, it is not easy to get satisfactory performance of PI/PID controller in the presence of uncertainties and variation of operating points due to wearing out of components. Further, the performance of fixed gain controllers will mortify in the existence of system nonlinearities and/or over loading condition. As fuzzy logic controller (FLC) can take care of deviation in system parameters and nonlinearities of practical system efficiently, the system performance can be enhanced via FLC [25–34]. Moreover, in the recent literature hybridized fuzzy-conventional controller structures are recommended to upgrade the performance of AGC in practical nonlinear electric power systems [25–34]. The selection of FLC parameters e.g., input scaling factors (SFs), output SFs, type of membership functions, formulation of rules etc., is an obscure task. Typically, these parameters are selected based on some empirical rules and usually may not be the best ones [25,26]. Their incorrect selection might influence the system performance negatively. Various optimization techniques have been profitably engaged to select the best parameters of fuzzy controllers such as adaptive SOS (ASOS) based fuzzy PID (FPID)/FPIDF [26], GA based fuzzy PI (FPI) [27], PSO based FPI [30], BFOA based FPI/FPID [31], FA based FPIDF [32] and ICA based FPI/FPIDF plus double integral (FPIDF-II)/fractional order FPID (FOFPID) [28,29,33,34] structured controllers for solving AGC problem in power system. However, widespread method of FLC optimization is to optimize its input/output SFs as they influence the performance of FLC greatly and additionally, it is a simple and economic method [26,27,29,31–34].

1.3. Motivation

As per the above literature survey, it is observed that AGC system outcome largely depends on the energy storage system, the configuration of the controller and the technique adopted for selecting the controller parameters. There are number of methods extant in the literature for tuning of AGC controllers. ICA is utilised in the existing researches due to its high convergence speed and veracity in obtaining the solutions of tuning problems. It is a newly developed socio-politically prompted optimization technique which is inspired by socio-political progression of Imperialism. ICA based FL controllers manifest robustness to handle parameter ambiguity and offer better stability/performance [28,29,33,34]. Further, it is observed that FPI, FPID, FPIDF, FPIDF-II and FOFPID configured optimized FL controllers are employed recently in AGC. A multi-stage optimized conventional controller having PDF controller to enhance the transient response characteristics and negate the derivative kick of D controller in the first stage and (1 + PI) controller in the second stage to eliminate the steady state error in the system response is proposed for AGC in Ref. [24]. Motivated by the above discussion, in this paper, a multi-stage ICA optimized fuzzy PIDF-(1 plus PI) i.e., FPIDF-(1 + PI) controller is proposed with CES units for the first time for AGC problem solution of power system models prevalent in the literature. The proposed multi-stage controller comprises of FLC, PIDF and (1 + PI) controllers in first, second and third stages, respectively. The simulation results reveal the efficiency of the proposed control scheme, which diminishes the frequency and tie-power deviations efficiently compared with the optimized conventional/fuzzy controller with/without CES and hence, offers quality and reliable electric power.

1.4. Contributions

The main contributions of present work are as follows:

(i) To propose an ICA optimized multi-stage FPIDF-(1 + PI) controller for AGC of two-area PV-reheat thermal power system model.
(ii) To demonstrate the advantage of the proposed controller over ICA optimized FPI/FPIDF controller and GA/FA/PEO optimized PI controller.
(iii) To authenticate the benefit of CES in suppressing the oscillations caused due to sudden load disturbance in control area-2 of the system stated in (i).
(iv) To implement the proposed controller on a two-area multi-unit multi-source hydro-thermal power system.
(v) To illustrate the superiority of the proposed controller over PID/FPI/FPID structured controller optimized using recently published hFA-PS/hGGSA-PS/BFOA/SOS/ASOS/ICA technique.
(vi) To investigate the efficacy and robustness of the proposed FPIDF-(1 + PI) controller with/without CES units over FPIDF under wide variations in the system parameters and random load demand.

Additionally, in order to make the proposed method more perceivable to the readers, a schematic overview of the whole paper has been showcased in Fig. 1.

1.5. Organisation of the paper

The rest of the paper is organised in these categorizations: In Section 2, the power system models simulated in the study are described. The modeling of capacitive energy storage is formulated in Section 3. Section 4 concentrates on the design of the proposed ICA optimized FPIDF-(1 + PI) controller. Simulation results are offered and analysed in Section 5. Section 6 focusses on conducting a sensitivity analysis of the proposed approach. Finally, conclusions and scope of future work are briefed in Section 7.

2. Power system models

The power systems considered in the study are two-area photovoltaic (PV)-reheat thermal system shown in Fig. 2 and a two-area multi-unit multi-source hydro-thermal power system shown in Fig. 3. MATLAB/SIMULINK version R2007b is used for codings and models of the systems. The study is conducted on application of a step load perturbation (SLP) in a control area. The nomenclature utilised is provided in Nomenclature section. The detailed mathematical modeling of the system models under study is depicted in Refs. [9,18,29,31,33,36]. The system data used in the simulations are provided in Appendix.

3. Modeling of capacitive energy storage (CES)

Due to the great potential in modern power system applications, CES devices are inviting attention in theoretical and experimental studies. They have the potential to alleviate low frequency power fluctuations and to stabilize system frequency deviations appeared as a result of system transients. Various advantage of CES such as

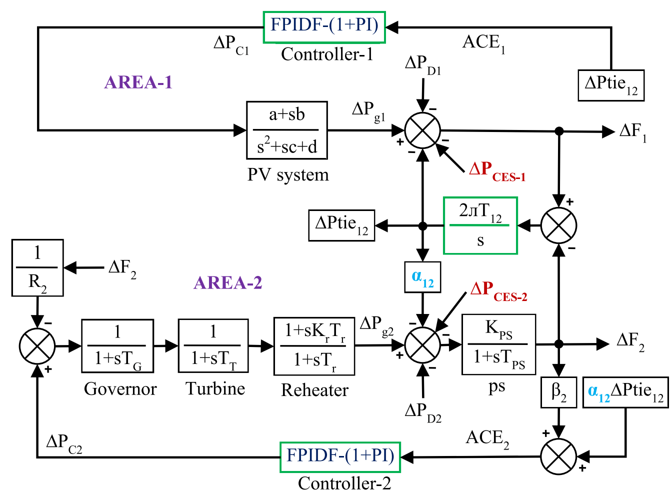

Fig. 2. Transfer function model of two-area PV-reheat thermal power system [18].

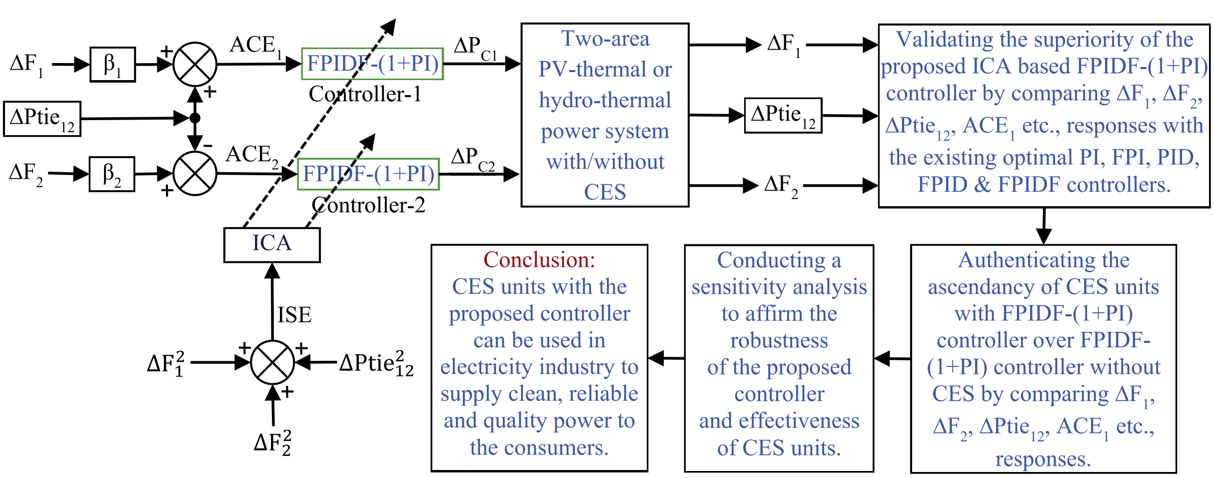

Fig. 1. Schematic overview of the proposed work.

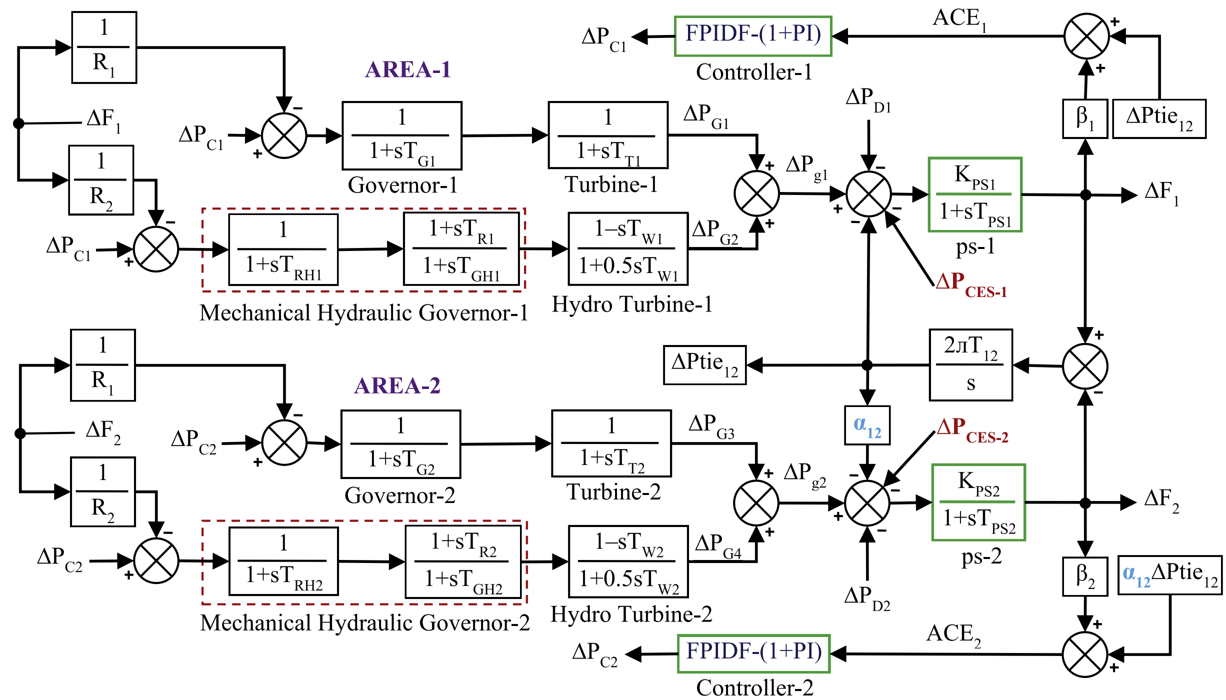

Fig. 3. Transfer function model of two-area multi-unit multi-source hydro-thermal power system [33].

quick charge/discharge rate without loss of efficiency, less response time, elevated power density, elongated working life, voluminous capability to supply high/intermittent power demand into the grid, don't require maintenance, environmental friendly, simple and less expensive operation etc. [3,4].

The CES unit comprises of a capacitor (a cryogenic hyper capacitor or a super capacitor), power conversion system (PCS) and associated protective circuitry [4]. CES unit stores energy during normal operating conditions and instantaneously releases it in to the grid via PCS under any sudden load demand. Therefore, CES aid AGC to regulate the power system hastily to the new equilibrium steady state condition. The energy efficiency of CES unit is approximately 95% [4]. Some losses are due to the PCS, internal leakage and self-discharge. Consequently, CES is an outstanding energy storage device to enhance the stability of an AGC system. Fig. 4 shows the transfer function model of a CES unit as a frequency stabilizer [4]. To guarantee the enhancement in dynamic performance of the power system and to alleviate the frequency and tie-line power deviations, CES units are integrated in both areas of the power system models under study. The incremental change in the power of CES unit is given as:

$$\Delta P_{CES-i} = \left\{ \left[\frac{1+sT_1}{1+sT_2}\right] \left[\frac{1+sT_3}{1+sT_4}\right] \left[\frac{K_{CES}}{1+sT_{CES}}\right] \right\} \Delta F_i \tag{1}$$

where i = 1, 2. T_1, T_2, T_3 and T_4 are the time constants of two-stage phase compensation blocks. K_{CES} denotes the gain and T_{CES} is the time constant of CES unit [4]. ΔF is the frequency deviation signal of an area. ΔF signal of each area is used as an input to CES unit meant to supply the requisite amount of power related to ΔF.

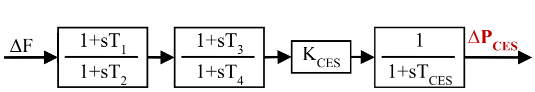

Fig. 4. Linearized model of CES as a frequency stabilizer [4].

4. Design of multi-stage FPIDF-(1 + PI) controller

The structure of the proposed multi-stage FPIDF-(1 + PI) controller is shown in Fig. 5(a). Similar controllers are employed in both areas of two-area systems under study. The FLC uses area control error (ACE) and derivative of ACE as input signals and its output y is multiplied with PIDF controller in second stage to get FPIDF controller. The output of second stage is multiplied with (1 + PI) controller to get final output ΔP_C of the proposed FPIDF-(1 + PI) controller as shown in Fig. 5(a). The control signals of FPIDF and the proposed controller are provided in Eqns. (2) and (3) and expressions of ACEs for both areas are depicted in Eqns. (4) and (5).

$$\Delta P_C = K_P y + \frac{K_I}{s} y + K_D y \left(\frac{sN_C}{s+N_C}\right) (\text{FPIDF controller}) \tag{2}$$

$$\Delta P_C = \left\{ K_P y + \frac{K_I}{s} y + K_D y \left(\frac{sN_C}{s+N_C}\right) \right\} \times \left\{ 1 + K_{P1} + \frac{K_{I1}}{s} \right\} \quad (\text{FPIDF} - (1+\text{PI})\ \text{controller}) \tag{3}$$

$$ACE_1 = \beta_1 \Delta F_1 + \Delta Ptie_{12} \tag{4}$$

$$ACE_2 = \beta_2 \Delta F_2 + \alpha_{12} \Delta Ptie_{12} \tag{5}$$

Here, K_P/K_{P1}, K_I/K_{I1}, K_D and N_C are proportional, integral, derivative and derivative filter gains, respectively. The β_1/β_2, $\Delta F_1/\Delta F_2$, $\Delta Ptie_{12}$ and α_{12} are frequency response characteristics, deviation in area frequency, deviation in tie-line power flow and area rating ratio, respectively.

A FLC comprises of four chief controls: fuzzification interface, rule base, fuzzy inference system (FIS) logic and defuzzification interface. The fuzzification interface changes binary values into fuzzy ones and the defuzzification interface does the contrary by means of membership function (MF). The rule base, a collection of IF-THEN rules illustrates the control approach. The output from

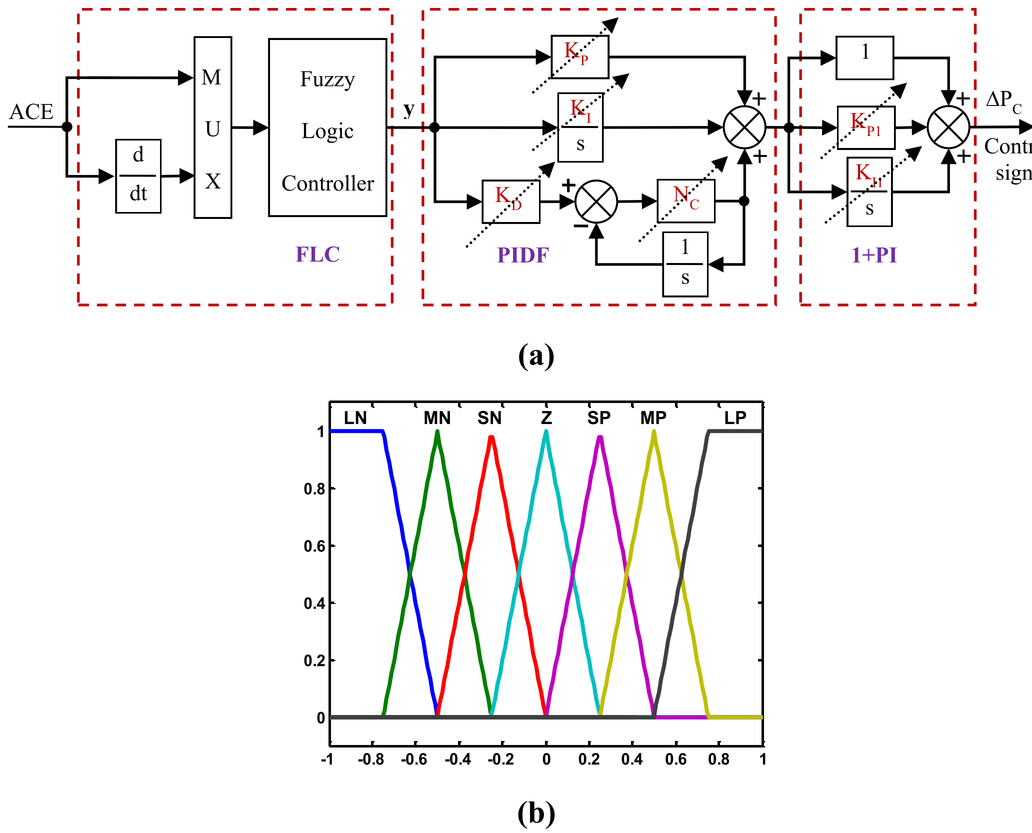

Fig. 5. Proposed controller. (a) Components of FPIDF-(1 + PI) controller and **(b)** membership functions for ACE, ACE derivative and FLC output [33].

each rule in the rule base is realized by FIS logic to arrive at a value for each output MF [28]. In the FLC, 7 MFs, 5 triangular (inner) and 2 trapezoidal (outermost) are employed for both inputs and one output with 7 linguistic variables: LN (Large Negative), MN (Medium Negative), SN (Small Negative), ZE (Zero), SP (Small Positive), MP (Medium Positive) and LP (Large Positive). The horizontal axis range of MFs is taken nominal from −1 to +1 for all three sets of MFs as shown in Fig. 5(b). The two-dimensional rule base for ACE, derivative of ACE and FLC output is shown in Table 1. These rules are attained by logic and analysis. Fuzzy rule 1 is expressed as follows:

Rule 1: IF ACE is LN and $\dot{\text{ACE}}$ is LN; THEN output is LP.

Where, LN denotes the antecedents and LP is the consequent part of the rule. The firing power of the rule base is accomplished via Mamdani FIS and centre of gravity method of defuzzification is used for conversion of FLC output fuzzy set to a crisp value.

The performance of the designed FPIDF-(1 + PI) controller depends on its parameters K_P, K_I, K_D, N_C, K_{P1} and K_{I1}. Therefore, in designing FPIDF-(1 + PI) controller, these parameters must be selected judiciously to attain the fruitful dynamic performance of the system. In this paper, a newly developed optimization technique termed imperialist competition algorithm (ICA) is employed to achieve the best values of the controller parameters. ICA is observed in various existing papers due to its high speed and precision in obtaining the solutions of optimization problems. It is a novel socio-politically instigated global search algorithm to deal with diverse optimization problems and it demonstrates great performance in both convergence rate and global optima attainment. It starts with an initial population. Each entity of the population is termed as a country and the best countries act as imperialist states. Others construct the colonies of these imperialists. These colonies of initial countries are distributed among the imperialists as per their power. The imperialist's power is inversely proportional to its cost. The imperialist states with their colonies form empires and then the colonies in each empire start gravitating towards their relevant imperialist country. The imperialistic competitions converge to a state where only one empire exists and its colonies occupy the same position and have the equal value for the imperialist. The more detailed theory of ICA has been described in the related literature [23,29,33–35].

Table 1
Rule base for ACE, ACE derivative and FLC output.

ACE	ACE derivative						
	LN	MN	SN	Z	SP	MP	LP
LN	LP	LP	LP	MP	MP	SP	Z
MN	LP	MP	MP	MP	SP	Z	SN
SN	LP	MP	SP	SP	Z	SN	MN
Z	MP	MP	SP	Z	SN	MN	MN
SP	MP	SP	Z	SN	SN	MN	LN
MP	SP	Z	SN	MN	MN	MN	LN
LP	Z	SN	MN	MN	LN	LN	LN

To optimize the controller parameters, a widely adopted cost function (J) in industry named integral squared error (ISE) defined via Eqn. (6) is used.

$$J = \int_0^T \left\{ \Delta F_1^2 + \Delta F_2^2 + \Delta Ptie_{12}^2 \right\} dt \tag{6}$$

T is the simulation time range. To get the best system performance, Eqn. (6) has minimum value. In order to optimize the different parameters of the controller, J is subjected to the limits of all the parameters. The controller optimization chore can be defined as the following constrained optimization problem. Minimize J subject to:

$$\left.\begin{array}{l} K_P^{min} \le K_P \le K_P^{max} \\ K_I^{min} \le K_I \le K_I^{max} \\ K_D^{min} \le K_D \le K_D^{max} \\ N_C^{min} \le N_C \le N_C^{max} \\ K_{P1}^{min} \le K_{P1} \le K_{P1}^{max} \\ K_{I1}^{min} \le K_{I1} \le K_{I1}^{max} \end{array}\right\} \tag{7}$$

In Eqn. (7), symbols min and max are the minimum and maximum values of the respective parameters. The parameters of ICA are chosen as: no of iterations = 100, no of countries = 500, no of initial empires = 40; no of initial colonies = 500–40 = 460; revolution rate = 0.3, coefficient associated with average power of empire's colonies = 0.05, assimilation coefficient = 1.5 and assimilation angle coefficient = 0.5. The optimization process is repeated 50 times and the best final values among the 50 runs are chosen as the parameters of the controller. The optimal values of $K_P/K_I/K_D/N_C/K_{P1}/K_{I1}$ of the proposed FPIDF-(1 + PI) controllers for two-area PV-reheat thermal and two-area multi-unit multi-source hydro-thermal system models in the presence/absence of CES units are provided in Table 2.

5. Simulation results

In the current study, the simulations are conducted on an Intel core i5-6200U CPU, 2.3 GHz and 8 GB RAM computer using MATLAB/SIMULINK version R2007b. The applicability of the proposed control approach is tested on two existing test systems. The simulation results are ruminated upon in the following subsections. The parameters of the test systems used in the study are provided in Appendix. The results of interest are bold faced in the relevant tables.

5.1. Two-area PV-reheat thermal system

The proposed control technique is initially implemented on a two-area photovoltaic (PV)-reheat thermal system selected from Ref. [18]. The configuration of the system is shown in Fig. 2. Area-1 of the system owns a PV system and area-2 has a reheat thermal system. The PV cell model consists of sunlight intensity dependent photovoltaic current source parallel with a diode and a small series contact resistance [18]. The complete transfer function of the PV system with PV panel, maximum power point tracking (MPPT), inverter and filters used in this study is detailed in Refs. [18,36]. The deviation in radiation and temperature is modeled as SLP in the PV system.

The system results of deviation in area-1 frequency (ΔF_1), deviation in area-2 frequency (ΔF_2) and deviation in tie-line power ($\Delta Ptie_{12}$) due to the proposed ICA optimized FPIDF-(1 + PI) controller and some other prevalent controllers such as GA/FA optimized PI [18], PEO optimized PI [9] and ICA optimized FPI [29]/FPIDF [33] under 10% SLP used in area-2 (i.e., $\Delta P_{D2} = 0.1$ puMW) at t = 0 s are demonstrated in Fig. 6(a–d). The numerical values of ISE cost function (J) and settling time (T_S), peak undershoot (U_S) of $\Delta F_1/\Delta F_2/\Delta Ptie_{12}$ response calculated during the simulation are tabled in Table 3. Fig. 6(a–c) and Table 3 indicate that better/minimum values of J (ISE = 0.0032), T_S (ΔF_1 = 12.33 s, ΔF_2 = 12.34 s, $\Delta Ptie_{12}$ = 1.91 s) and U_S (ΔF_1 = −0.0435 Hz, ΔF_2 = −0.0434 Hz, $\Delta Ptie_{12}$ = −0.0005 puMW) are offered by the proposed FPIDF-(1 + PI) controller compared to the existing GA/FA: PI [18], PEO: PI [9] and ICA: FPI [29]/FPIDF [33] controllers. However, the performance of the proposed controller is further improved in the presence of CES units incorporated in the control areas. With CES, it shows the lowest J (ISE = 0.0004), T_S (ΔF_1 = 8.19 s, ΔF_2 = 8.20 s, $\Delta Ptie_{12}$ = 1.58 s) and U_S (ΔF_1 = −0.0169 Hz, ΔF_2 = −0.0166 Hz, $\Delta Ptie_{12}$ = −0.0001 puMW) values. Further, it is apparent from Fig. 6(d) that the transient oscillations in tie-line power deviation signal are significantly damped out and settle very quickly with the proposed controller in the presence of CES.

To support the proposed approach effectively, the simulation results are extended by including the responses of area-2 area control error (ACE_2), area-1 power generation (ΔP_{g1}) and area-2 power generation (ΔP_{g2}) in Fig. 6(e–g) and Table 4. It is observed from Fig. 6(e–g) that with the proposed method $ACE_2/\Delta P_{g1}$ driven back to zero position and ΔP_{g2} achieves required 0.1 puMW of power generation (i.e., equal to load demand in thermal area) in minimum time, with minimum undershoots and minimum oscillations as indicated in Table 4. Fig. 6(e–g) and Table 4 also demonstrate the excellence of CES units. Hence, the efficacy of CES in alleviating the oscillations in power system at dynamic condition is validated. So, the suggested controller provides the desired performance both in the presence or absence of CES units.

It should be noted that T_S of simulation results in the current study is calculated considering a tolerance band of ±0.0005 and ISE for a simulation time of 15 s for both the test system models under study [27,29,33,34].

5.2. Two-area multi-unit multi-source hydro-thermal system

A two-area multi-unit multi-source hydro-thermal system is simulated to decipher the capability, scalability and excellency of the proposed control method and CES units in multi-unit multi-source system. The transfer function model of the system is displayed in Fig. 3. Each area of Fig. 3 is outfitted with two units, one non-reheat thermal unit and other mechanical governor based hydro unit. The ΔF_1, ΔF_2 and $\Delta Ptie_{12}$ responses of the system for 1.5% SLP in area-1 applied at t = 0 s using the proposed controller are shown in Fig. 7(a–c) and Table 5. To compare the proposed controller performance, the simulation results due to the existing hFA-PS based PID [21], hGGSA-PS based PID [17], SOS/ASOS based PID [26], BFOA based FPI/FPID [31] and ICA based FPIDF [33] controllers are also incorporated in these figures and Table 5. It is revealed from the study of these figures and Table 5 that the proposed controller outperforms the other controllers decently. It is observed that the minimum values of J (ISE = 2.49e^{-6}), T_S (ΔF_1 = 0.60 s, ΔF_2 = 1.25 s, $\Delta Ptie_{12}$ = 0.52 s) and U_S (ΔF_1 = −0.0027 Hz, ΔF_2 = −0.0007 Hz, $\Delta Ptie_{12}$ = −0.00029 puMW) are obtained due to the proposed controller compared to the other existing methods. The impact of CES demonstrates its effectiveness via further reducing $J/T_S/U_S$ or enhancing the outcome of the proposed controller.

Some additional system results of ACE_1, ΔP_{g1} and ΔP_{g2} states are also illustrated in Fig. 7(d–f) and Table 6. Results specify that the proposed ICA tuned FPIDF-(1 + PI) controller with/without CES

Table 2
Optimized FPIDF-(1 + PI)/FPIDF-(1 + PI)-CES controller parameters.

Controller parameters	PV-reheat thermal system		Multi-unit multi-source hydro-thermal system	
	FPIDF-(1 + PI)	FPIDF-(1 + PI)-CES	FPIDF-(1 + PI)	FPIDF-(1 + PI)-CES
K_P	1.3654	2.5264	1.4532	2.2467
K_I	2.9621	5.6523	4.8351	9.8642
K_D	0.3584	0.7357	0.1024	0.1352
N_C	354.5842	413.6852	351.6324	10.5328
K_{P1}	1.0634	1.5314	1.3543	1.1351
K_{I1}	0.0324	0.0092	0.1059	0.0234

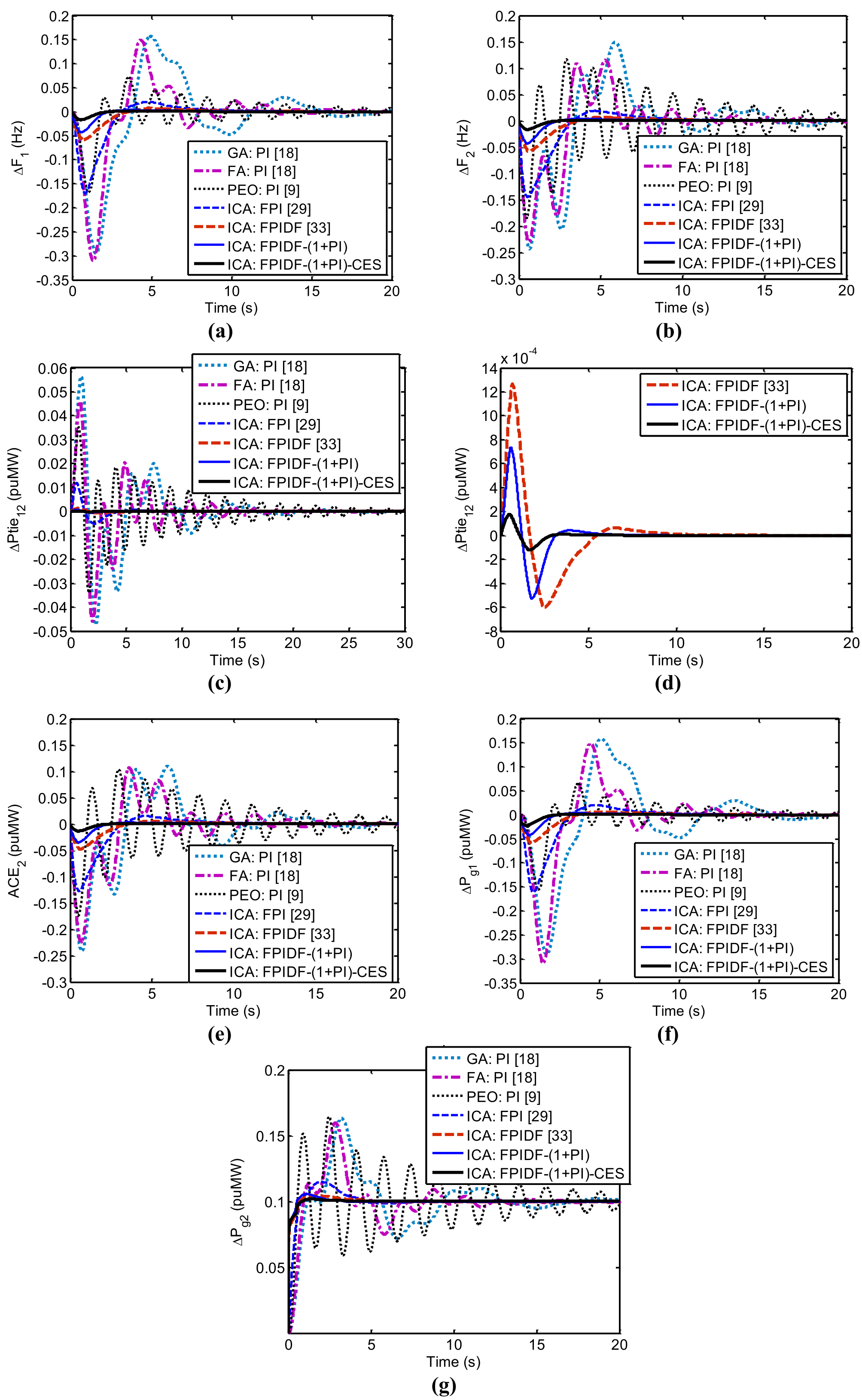

Fig. 6. Responses of two-area PV-reheat thermal power system for $\Delta P_{D2} = 0.1$ puMW. (a) ΔF_1, (b) ΔF_2, (c) $\Delta Ptie_{12}$, (d) Fig. (c) with/without CES showing more clarity, (e) ACE_2, (f) ΔP_{g1} and (g) ΔP_{g2}.

Table 3
Numerical values of $T_S/U_S/J$ with PV-reheat thermal system.

Control strategy	T_S (s)			U_S (−ve) (Hz)		U_S (−ve) (puMW)	J
	ΔF_1	ΔF_2	$\Delta Ptie_{12}$	ΔF_1	ΔF_2	$\Delta Ptie_{12}$	ISE
GA: PI [18]	30.33	30.25	23.19	0.2941	0.2437	0.0474	0.2710
FA: PI [18]	25.76	26.91	20.58	0.3109	0.2308	0.0460	0.1998
PEO: PI [9]	42.84	49.53	35.20	0.1687	0.1841	0.0339	0.0797
ICA: FPI [29]	16.34	16.35	6.40	0.1699	0.1446	0.0051	0.0563
ICA: FPIDF [33]	14.27	14.28	3.00	0.0590	0.0583	0.0006	0.0085
ICA: FPIDF-(1 + PI)	12.33	12.34	1.91	0.0435	0.0434	0.0005	0.0032
ICA: FPIDF-(1 + PI)-CES	**8.19**	**8.20**	**1.58**	**0.0169**	**0.0166**	**0.0001**	**0.0004**

Table 4
Numerical values of T_S/U_S with PV-reheat thermal system.

Control strategy	T_S (s)			U_S (puMW)		
	ACE_2	ΔP_{g1}	ΔP_{g2}	ACE_2 (−ve)	ΔP_{g1} (−ve)	ΔP_{g2} (+ve)
GA: PI [18]	29.87	30.52	24.14	0.2415	0.2904	0.0281
FA: PI [18]	25.23	24.24	19.73	0.2243	0.3082	0.0250
PEO: PI [9]	47.21	41.34	42.59	0.1738	0.1566	0.0411
ICA: FPI [29]	15.56	16.37	7.70	0.1274	0.1613	0.0015
ICA: FPIDF [33]	13.52	14.28	4.69	0.0479	0.0577	0.0002
ICA: FPIDF-(1 + PI)	11.29	12.34	3.34	0.0354	0.0428	0.0001
ICA: FPIDF-(1 + PI)-CES	**7.41**	**8.99**	**3.33**	**0.0135**	**0.0241**	**0**

units demonstrates smoother response with much smaller settling time compared to hFA-PS/hGGSA-PS/SOS/ASOS tuned PID, BFOA tuned FPI/FPID and ICA tuned FPIDF controllers. It exhibits less undershoots for ACE_1 and ΔP_{g1} responses. However, it does not show the best undershoots for ΔP_{g2} power generation. Moreover, in dynamic condition, the desired steady value of ACE_1 error/ΔP_{g2} generation demonstrates zero deviations and ΔP_{g1} generation equals to 0.015 puMW which is equal to the step load disturbance in area-1. Though, FPIDF-(1 + PI) highly establishes a better recital compared to the other controllers, specifically considering oscillations and settling time.

6. Sensitivity analysis

A sensitivity analysis is undertaken to inspect the robustness of the proposed ICA optimized FPIDF-(1 + PI) controller parameters under wide variations in the system parameters [15,20,21,26,27,29,31–34]. The system parameters change over the time. They also vary due to the variations in the configurations of the system. Considering this, the designed controller should be capable to execute robustly devoid of much decline in the system performance under broad changes in the system parameters. Fig. 8(a) shows $\Delta Ptie_{12}$ response at nominal and ±25% simultaneous change in nominal (1/R), T_G, T_T, K_{PS} and T_{PS} parameters of two-area PV-reheat thermal system and Fig. 8(b) shows ΔF_2 response at nominal and ±25% simultaneous change in nominal R_1, T_R, T_{GH} and T_W parameters of two-area multi-unit multi-source hydro-thermal system. Fig. 8(a and b) include results due to FPIDF, FPIDF-(1 + PI) and FPIDF-(1 + PI) with CES. The critical inspection of Fig. 8(a and b) unveils that all the responses are more or less same under extensive changes in the parameters of the systems. Fig. 8(a and b) also confirm the superiority of FPIDF-(1 + PI) over FPIDF controller.

To illustrate the vigorousness and superiority of the proposed method further, a random load pattern is applied in control area-1 of two-area PV-reheat thermal and multi-unit multi-source hydro-thermal power systems. If the controller is not robust enough, the system under random load pattern will turn unstable. ΔF_2 result of PV-reheat thermal and ΔF_1 result of multi-unit multi-source hydro-thermal systems acquired after simulations are depicted in Fig. 8(c) and (d), respectively. Here, performance of FPIDF is compared with the proposed FPIDF-(1 + PI) controller with/without CES. From dynamic responses, it is observed that the proposed controller achieves excellent and robust performance following variable load change pattern. So, the proposed approach executes robustly under changed system parameters and hence, the controller optimized at nominal operating condition needs not be tuned again at changed operating conditions.

7. Conclusions and scope of future work

7.1. Conclusions

In this paper, the impact of CES in AGC performance enrichment of power system is analysed critically. A new ICA optimized multi-stage FPIDF-(1 + PI) controller is proposed as an intelligent and proficient supplementary controller to deal with AGC problem of power system efficiently. The efficacy of the proposed control strategy is validated on two-area PV-reheat thermal and multi-unit multi-source hydro-thermal power system models prevalent in the literature. The following are the significant conclusions of the present research work:

i) The proposed ICA optimized FPIDF-(1 + PI) controller provides better performance in comparison to the existing best acknowledged GA/FA/PEO optimized PI, hFA-PS/hGGSA-PS/SOS/ASOS optimized PID, BFOA optimized FPI/FPID and ICA optimized FPI/FPIDF controllers in terms least values of oscillations/T_S/U_S/J.
ii) Application of CES units alleviate system oscillations excellently following a step load disturbance in any control area of the power system as FPIDF-(1 + PI) controller with CES units offers superior performance than FPIDF-(1 + PI) controller without CES units.
iii) Fuzzy controller with fixed structure of MFs and rule base having optimized SFs is easy to implement; and provides acceptable and bankable performance. Additionally, it can be exploited for a reasonably extensive class of power systems.

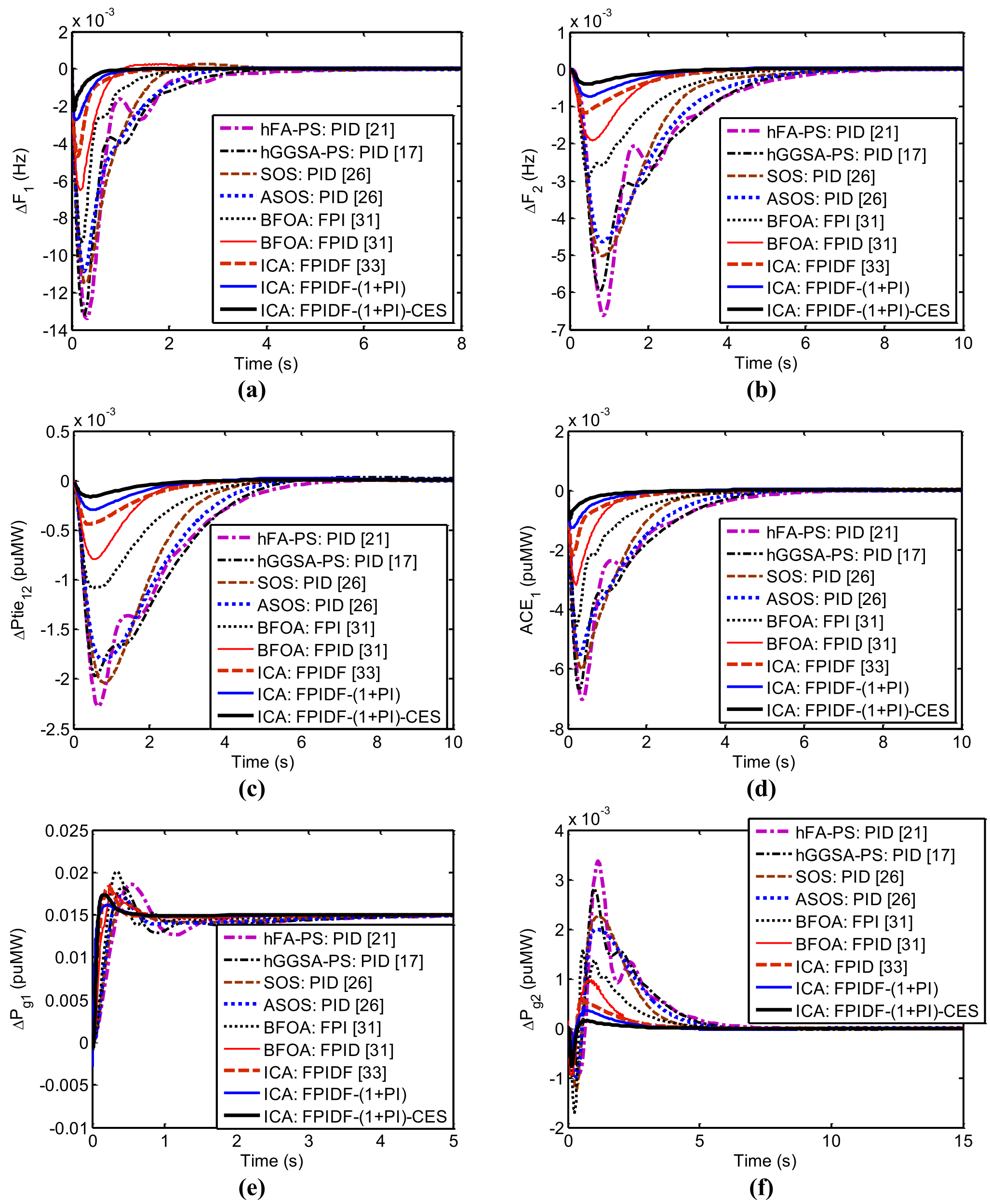

Fig. 7. Responses of two-area multi-unit multi-source hydro-thermal power system for $\Delta P_{D1} = 0.015$ puMW. (a) ΔF_1, (b) ΔF_2, (c) $\Delta Ptie_{12}$, (d) ACE_1, (e) ΔP_{g1} and (f) ΔP_{g2}.

Table 5
Numerical values of $T_S/U_S/J$ with multi-unit multi-source hydro-thermal system.

Control strategy	T_S (s)			U_S (−ve) (Hz)		U_S (−ve) (puMW)	J
	ΔF_1	ΔF_2	$\Delta Ptie_{12}$	ΔF_1	ΔF_2	$\Delta Ptie_{12}$	ISE
hFA-PS: PID [21]	2.94	4.53	3.30	0.0134	0.0066	0.00220	1.17×10^{-4}
hGGSA-PS: PID [17]	2.70	4.38	3.37	0.0132	0.0059	0.00197	1.11×10^{-4}
SOS: PID [26]	1.75	3.23	2.64	0.0115	0.0050	0.00203	1.01×10^{-4}
ASOS: PID [26]	2.29	3.96	3.04	0.0109	0.0046	0.00180	8.94×10^{-5}
BFOA: FPI [31]	1.41	2.86	1.92	0.0093	0.0029	0.00108	3.47×10^{-5}
BFOA: FPID [31]	0.82	1.79	1.17	0.0065	0.0019	0.00079	1.60×10^{-5}
ICA: FPIDF [33]	0.78	1.59	0.60	0.0047	0.0011	0.00043	6.01×10^{-6}
ICA: FPIDF-(1 + PI)	0.60	1.25	0.52	0.0027	0.0007	0.00029	2.49×10^{-6}
ICA: FPIDF-(1 + PI)-CES	**0.39**	**1.20**	**0.46**	**0.0022**	**0.0003**	**0.00016**	$\mathbf{8.19 \times 10^{-7}}$

iv) The proposed control strategy with/without CES units displays robust and favorable demeanor following variation in system parameters and random load demand patterns. It assures that the proposed FPIDF-(1 + PI) controller

Table 6
Numerical values of T_S/U_S with multi-source hydro-thermal system.

Control strategy	T_S (s)			U_S (puMW)		
	ACE_1	ΔP_{g1}	ΔP_{g2}	ACE_1 (−ve)	ΔP_{g1} (+ve)	ΔP_{g2} (−ve)
hFA-PS: PID [21]	3.60	2.85	3.72	7.02×10^{-3}	2.40×10^{-3}	9.14×10^{-4}
hGGSA-PS: PID [17]	3.52	3.26	3.66	6.66×10^{-3}	2.10×10^{-3}	7.53×10^{-4}
SOS: PID [26]	2.48	2.61	2.97	5.99×10^{-3}	8.00×10^{-4}	1.24×10^{-3}
ASOS: PID [26]	3.08	2.88	3.34	5.52×10^{-3}	1.10×10^{-3}	9.98×10^{-4}
BFOA: FPI [31]	2.08	1.61	2.29	4.54×10^{-3}	1.20×10^{-3}	1.69×10^{-3}
BFOA: FPID [31]	1.11	0.63	1.54	3.16×10^{-3}	4.00×10^{-4}	9.52×10^{-4}
ICA: FPIDF [33]	0.94	0.41	0.74	2.19×10^{-3}	2.01×10^{-4}	7.89×10^{-4}
ICA: FPIDF-(1 + PI)	0.60	0.40	0.70	1.26×10^{-3}	1.99×10^{-4}	4.70×10^{-4}
ICA: FPIDF-(1 + PI)-CES	**0.25**	**0.38**	**0.66**	$\mathbf{9.89 \times 10^{-4}}$	$\mathbf{1.00 \times 10^{-4}}$	7.80×10^{-4}

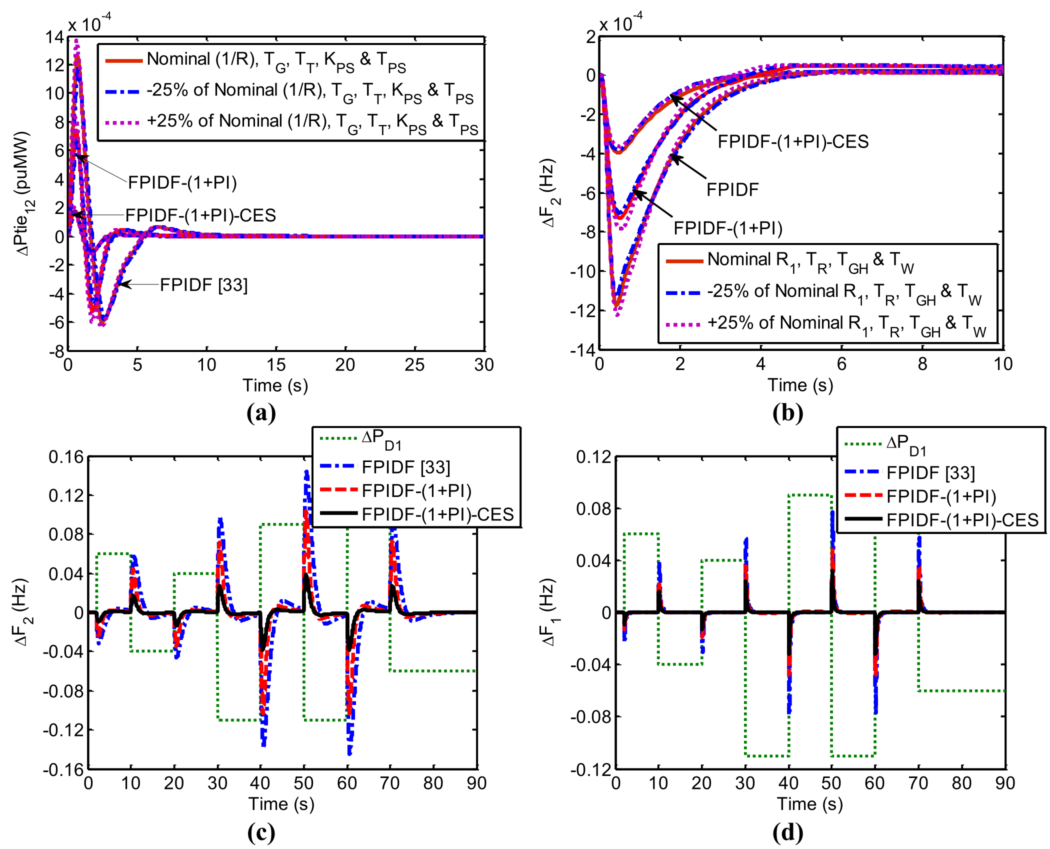

Fig. 8. *Responses under sensitivity analysis.* (a) $\Delta Ptie_{12}$ of PV-reheat thermal system, (b) ΔF_2 of multi-unit multi-source hydro-thermal system, (c) ΔF_2 of PV-reheat thermal system at random load and (d) ΔF_1 of multi-unit multi-source hydro-thermal system at random load.

parameters optimized via ICA may be able in handling the huge range of variation in the system parameters and disturbances.

v) The application of ICA is fruitful in extracting the near-global optimal solution of the studied power systems optimization task.

7.2. *Scope of future work*

As scope of future work, the following points may be put forward:

i) The current study can be extended in the near future to the large traditional and restructured multi-area power systems equipped with more types of renewable power sources.

ii) In the present study, the impact of CES on power system performance is analysed. In further studies, the impact of some other energy storage devices like ultra-capacitor (UC), battery energy storage system (BESS), redox flow battery (RFB), flywheel energy storage system (FESS) etc., can be scrutinised in renewable power systems.

iii) The implementation of the proposed controller in some other control systems may inspire prospective researchers.

iv) In the current study, the proposed controller is optimized via ICA. In future, some other optimization techniques like whale optimization algorithm (WOA), stochastic fractal search (SFS), sine-cosine algorithm (SCA), lightning search algorithm (LSA) etc., can be adopted to optimize and compare performance of the proposed controller.

Appendix A. Supplementary data

Supplementary data to this article can be found online at https://doi.org/10.1016/j.renene.2018.11.071.

Appendix

Systems data:

Two-area PV-reheat thermal power system [9,18,29]:

$F^0 = 60$ Hz, $K_{PS} = 120$ Hz/puMW, $T_{PS} = 20$ s, $T_G = 0.08$ s, $K_r = 0.33$, $T_r = 10$ s, $T_T = 0.3$ s, $R = 2.5$ Hz/puMW, $\beta = 0.8$ puMW/Hz, $2\pi T_{12} = 0.545$ puMW/Hz, $\alpha_{12} = -1$, $a = 900$, $b = -18$, $c = 100$, $d = 50$.

Two-area multi-unit multi-source hydro-thermal power system [21,31,33]:

$F^0 = 60$ Hz, $K_{PSi} = 100$ Hz/puMW, $T_{PSi} = 20$ s, $T_{Gi} = 0.08$ s, $T_{Ti} = 0.3$ s, $R_1 = 2$ Hz/puMW, $R_2 = 2.4$ Hz/puMW, $\beta_i = 0.425$ puMW/Hz, $T_{12} = 0.0707$ puMW/rad, $T_{RHi} = 48.7$ s, $T_{Ri} = 5$ s, $T_{GHi} = 0.513$ s, $T_{Wi} = 1$ s, $\alpha_{12} = -1$.

References

[1] K.G. Boroojeni, M.H. Amini, S.S. Iyengar, Smart Grids: Security and Privacy Issues, Springer International Publishing, Switzerland, 2017.
[2] M. Nayeripour, M. Hoseintabar, T. Niknam, Frequency deviation control by coordination control of FC and double-layer capacitor in an autonomous hybrid renewable energy power generation system, Renew. Energy 36 (6) (2011) 1741–1746.
[3] S.C. Tripathy, Improved load-frequency control with capacitive energy storage, Energy Convers. Manag. 38 (6) (1997) 551–562.
[4] S. Dhundhara, Y.P. Verma, Capacitive energy storage with optimized controller for frequency regulation in realistic multisource deregulated power system, Energy 147 (2018) 1108–1128.
[5] R. Shankar, S.R. Pradhan, K. Chatterjee, R. Mandal, A comprehensive state of the art literature survey on LFC mechanism for power system, Renew. Sustain. Energy Rev. 76 (6) (2017) 1185–1207.
[6] A. Pappachen, A.P. Fathima, Critical research areas on load frequency control issues in a deregulated power system: a state-of-the-art-of-review, Renew. Sustain. Energy Rev. 72 (2017) 163–177.
[7] Y. Arya, N. Kumar, Optimal control strategy-based AGC of electrical power systems: a comparative performance analysis, Optim. Contr. Appl. Methods 38 (6) (2017) 982–992.
[8] Y. Arya, N. Kumar, S.K. Gupta, Load frequency control of a four-area power system using linear quadratic regulator, Int. J. Energy Sci. 2 (2) (2012) 69–76.
[9] G.-Q. Zeng, X.-Q. Xie, M.-R. Chen, An adaptive model predictive load frequency control method for multi-area interconnected power systems with photovoltaic generations, Energies 10 (11) (2017) 1840.
[10] H. Gozde, M.C. Taplamacioglu, Automatic generation control application with craziness based particle swarm optimization in a thermal power system, Int. J. Electr. Power Energy Syst. 33 (1) (2011) 8–16.
[11] B. Mohanty, S. Panda, P.K. Hota, Differential evolution algorithm based automatic generation control for interconnected power systems with non-linearity, Alexandria Eng. J. 53 (3) (2014) 537–552.
[12] P.K. Hota, B. Mohanty, Automatic generation control of multi source power generation under deregulated environment, Int. J. Electr. Power Energy Syst. 75 (2016) 205–214.
[13] A. Rahman, L.C. Saikia, N. Sinha, Automatic generation control of an interconnected two-area hybrid thermal system considering dish-stirling solar thermal and wind turbine system, Renew. Energy 105 (2017) 41–54.
[14] P. Dahiya, V. Sharma, R. Naresh, Automatic generation control using disrupted oppositional based gravitational search algorithm optimized sliding mode controller under deregulated environment, IET Gener., Transm. Distrib. 10 (16) (2016) 3995–4005.
[15] R.K. Sahu, S. Panda, U.K. Rout, D.K. Sahoo, Teaching learning based optimization algorithm for automatic generation control of power system using 2-DOF PID controller, Int. J. Electr. Power Energy Syst. 77 (2016) 287–301.
[16] H. Gozde, M.C. Taplamacioglu, I. Kocaarslan, Comparative performance analysis of artificial bee colony algorithm in automatic generation control for interconnected reheat thermal power system, Int. J. Electr. Power Energy Syst. 42 (1) (2012) 167–178.
[17] R.K. Khadanga, A. Kumar, Hybrid adaptive 'gbest'-guided gravitational search and pattern search algorithm for automatic generation control of multi-area power system, IET Gener., Transm. Distrib. 11 (13) (2017) 3257–3267.
[18] S.M. Abd-Elazim, E.S. Ali, Load frequency controller design of a two-area system composing of PV grid and thermal generator via firefly algorithm, Neural Comput. Appl. 30 (2) (2018) 607–616.
[19] T.S. Gorripotu, R.K. Sahu, S. Panda, Comparative performance analysis of classical controllers in LFC using FA technique, in: International Conference on Electrical, Electronics, Signals, Communication and Optimization (EESCO), Visakhapatnam, India, 2015.
[20] S. Padhan, R.K. Sahu, S. Panda, Application of firefly algorithm for load frequency control of multi-area interconnected power system, Elec. Power Compon. Syst. 42 (13) (2014) 1419–1430.
[21] R.K. Sahu, S. Panda, S. Padhan, A hybrid firefly algorithm and pattern search technique for automatic generation control of multi area power systems, Int. J. Electr. Power Energy Syst. 64 (2015) 9–23.
[22] D. Guha, P.K. Roy, S. Banerjee, Symbiotic organism search algorithm applied to load frequency control of multi-area power system, Energy Syst. 9 (2) (2018) 439–468.
[23] N. Kumar, V. Kumar, B. Tyagi, Multi area AGC scheme using imperialist competition algorithm in restructured power system, Appl. Soft Comput. 48 (2016) 160–168.
[24] R. Sivalingam, S. Chinnamuthu, S.S. Dash, A hybrid stochastic fractal search and local unimodal sampling based multistage PDF plus (1+PI) controller for automatic generation control of power systems, J. Franklin Inst. 354 (12) (2017) 4762–4783.
[25] Y. Arya, N. Kumar, S.K. Sinha, Fuzzy logic based load frequency control of multi-area electrical power system considering non-linearities and boiler dynamics, Int. Energy J. 13 (2) (2012) 97–111.
[26] J.R. Nayak, B. Shaw, B.K. Shahu, Application of adaptive-SOS (ASOS) algorithm based interval type-2 fuzzy-PID controller with derivative filter for automatic generation control of an interconnected power system, Eng. Sci. Technol. Int. J. 21 (3) (2018) 465–485.
[27] Y. Arya, N. Kumar, Fuzzy gain scheduling controllers for AGC of two-area interconnected electrical power systems, Elec. Power Compon. Syst. 44 (7) (2016) 737–751.
[28] S. Falahati, S.A. Taher, M. Shahidehpour, Grid frequency control with electric vehicles by using of an optimized fuzzy controller, Appl. Energy 178 (2016) 918–928.
[29] Y. Arya, Automatic generation control of two-area electrical power systems via optimal fuzzy classical controller, J. Franklin Inst. 355 (5) (2018) 2662–2688.
[30] V. Jeyalakshmi, P. Subburaj, PSO-scaled fuzzy logic to load frequency control in hydrothermal power system, Soft Comput. 20 (7) (2016) 2577–2594.
[31] Y. Arya, N. Kumar, Design and analysis of BFOA-optimized fuzzy PI/PID controller for AGC of multi-area traditional/restructured electrical power systems, Soft Comput. 21 (21) (2017) 6435–6452.
[32] G.T.C. Sekhar, R.K. Sahu, A.K. Baliarsingh, S. Panda, Load frequency control of power system under deregulated environment using optimal firefly algorithm, Int. J. Electr. Power Energy Syst. 74 (2016) 195–211.
[33] Y. Arya, AGC of two-area electric power systems using optimized fuzzy PID with filter plus double integral controller, J. Franklin Inst. 355 (11) (2018) 4583–4617.
[34] Y. Arya, AGC performance enrichment of multi-source hydrothermal gas power systems using new optimized FOFPID controller and redox flow batteries, Energy 127 (2017) 704–715.
[35] E. Atashpaz-Gargari, C. Lucas, Imperialist competitive algorithm: an algorithm for optimization inspires by imperialistic competition, in: IEEE Congress on Evolutionary Computation, Singapore, Sep. 25-28, 2007, pp. 4661–4667.
[36] F.T. Tomy, R. Prakash, Load frequency control of a two area hybrid system consisting of a grid connected PV system and thermal generator, Int. J. Res. Eng. Technol. 3 (7) (2014) 573–580.